

Atmospheric Correction Using 1240 and 2130 nm Combination of MODIS SWIR Channels

Nivedita Sanwani *, Prakash Chauhan and R. R. Navalgund

Space Applications Centre, (ISRO), Ahmedabad-380015, Gujarat, India.

Abstract

It is essential to improve understanding of coastal ocean since the majority of the world's primary production occurs on continental shelves and the coastal ocean is most utilized and impacted by humans. The first step in ocean-colour data processing is the removal of atmospheric contribution from the sensor-detected radiance to enable detection of optically active oceanic constituents e.g. chlorophyll-a, suspended sediment etc. Black ocean assumption at the near infrared (NIR) wavelengths as applied to perform atmospheric correction fails for coastal turbid waters due to the presence of highly scattering sediments which cause sufficient water-leaving radiance in NIR wavelengths and lead to over-estimation of aerosol radiance for $\lambda < 700\text{nm}$ resulting in negative water leaving radiance for $\lambda < 500\text{nm}$. The assumption of zero water-leaving radiance at the NIR wavelengths was replaced by the assumption of zero water-leaving radiance at the short wave infrared (SWIR) wavelengths over the coastal turbid waters and atmospheric correction was performed using these SWIR wavelengths. Physically realistic and positive water leaving radiances throughout the spectrum and especially for shorter wavelengths (412nm, 443nm, 490nm) were obtained over coastal turbid waters using this concept.

Key words: Atmospheric Correction, Ocean Colour, MODIS, NIR, SWIR

1. Introduction

The light reaching the satellite sensor originates from the sun. Remotely sensed signal over the ocean can be divided into three main components: light scattered by atmospheric molecules and aerosols; specularly reflected direct sunlight at the water surface; and light upwelling from the sea surface after being backscattered in the water. The latter component is carrying the useful information about the sea water constituents. In this context the other two components of the detected signal must be removed. The process of removing atmospheric effects on the recorded radiance and retrieving the surface reflectance is called atmospheric correction. In fact, atmospheric contribution accounts for more than 80% of the top of the atmosphere (TOA) signal (Morel 1980). Due to temporal and spatial variability of the types and amount of aerosol, quantifying the atmospheric contribution is a difficult task. The standard ocean color algorithm processing assumes, that Ocean is black at the near infrared (NIR) wavelengths and aerosols are non- or weakly absorbing

(Gordon and Wang 1994; Antoine and Morel 1999; Moore *et al.* 1999; Siegal, 2000; Chauhan *et al.*, 2002). This assumption is rendered invalid in the coastal regions where the water is mostly turbid due to river inputs, sediment suspension and re-suspension, and plankton blooms leading to significant NIR ocean contributions. The situation is further complicated over coastal waters, where the mixing of various types of aerosols frequently occur and presence of strongly absorbing aerosols from adjacent land areas. Here, the derived ocean color products have significant errors, like the derived normalized water-leaving radiance $nL_w(\lambda)$ at the shorter wavelengths (blue region of the spectrum) are biased low (Ruddick, 2000; Hu *et al.*, 2000; Lavender *et al.*, 2005). A lot of scientific efforts have therefore been invested in modeling the optical properties of the aerosols, as well as in the development of algorithms for atmospheric correction (Zhang *et al.*, 2002; Jamet *et al.*, 2004; Schroeder *et al.*, 2003). For identification of the sediment loaded turbid waters, Morel and Belanger (2006) refined the scheme and used $nL_w(\lambda)$ threshold values at the green wavelengths.

©2011 AARS, All rights reserved.

* Corresponding author: s.ndita@gmail.com

Tel: 07926914143, 07926914140

Nobileau and Antoine (2005) have evolved an algorithm for detecting strongly absorbing aerosols over open oceans based on the approach used by Antoine & Morel, 1999 for deriving $nL_w(\lambda)$ at 510 nm. Significantly large contributions from other constituents in green wavelengths made these algorithms unreliable for the detection of turbid waters. As against this, the absorbing aerosols issue can be solved by the satellite measurements at the ultraviolet (UV) wavelengths (Torres et. al., 1998) but the ocean color sensors (e.g., OCEANSAT, SeaWiFS, MODIS), currently in use; do not have the UV sensors. Use of shortwave infrared (SWIR) wavelengths for the detection of turbid waters has been demonstrated by Gao et. al., (2000) and Li et. al., (2003) where water has much stronger absorption than that at NIR wavelengths and reflectance from turbid productive waters can be assumed to be zero. Hence, these channels are mainly influenced by aerosol scattering and absorption and can be used to derive atmospheric spectral law for atmospheric correction.

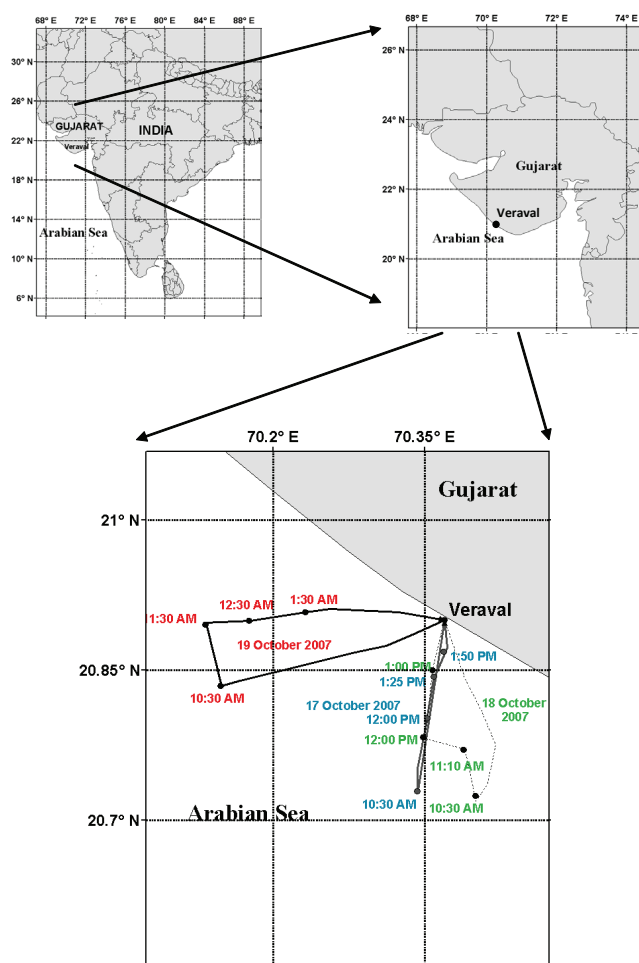


Figure 1. Geographical distribution of the sampling stations and the cruise track during 17th -19th October 2007 for collecting the bio-optical data in the coastal waters Off Veraval, Gujarat.

2. Study Area

Veraval a fishing harbour of Gujarat, India, is situated at latitude $20^{\circ}54'40''$ and longitude $70^{\circ}22'12''$ E on the South West coast of Saurashtra peninsula facing Arabian Sea. The port is well protected by breakwater extending 160 ft (Approx. 48 m) in the open sea with fairly deep water of about 8 to 9 fathoms. Pollution load, due to boats and vessels, domestic wastewater emanating from the Veraval town and effluent generation by about 42 fish processing industries gets discharged into this fishing harbour area. All these sources from different spheres subsequently contaminate the coastal waters. Figure 1 shows the geographical distribution of the station locations and cruise track during the study period.

3. Data Used

3.1 MODIS-Aqua satellite data

MODIS-Aqua has thirty six spectral channels, on-board calibration facility and capability of simultaneous observations of ocean colour and sea surface temperature with global coverage of alternate day. The nine channels ranging from 412 to 869 nm are intended for ocean color remote sensing (Esaias et. al., 1998). MODIS SWIR bands at wavelengths 1240, 1640, and 2130 nm are originally designed for land and atmosphere applications.

3.2 In-situ data

In-situ bio-optical measurements were done using SATLANTIC hyper-spectral under-water radiometer during 17-19th, October 2007 onboard *Sagar-Kripa* covering wide variety of highly productive waters off Veraval. Upwelling water-leaving radiance (L_w), down-welling irradiance (E_d), surface irradiance (E_s) measurements for 350-800nm with 2nm spectral interval and Chl-*a* concentration in 3 days at 12 stations were recorded. These have been used to compute L_w and R_{rs} by use of well-known equations.

4. Methodology

In the ocean-colour remote sensing, the total signal received at the satellite altitude, is considerably affected by radiance contribution through atmospheric scattering processes, so much so that, only 8–10% of the signal corresponds to oceanic radiance. Therefore, it becomes necessary to correct these atmospheric effects so as to estimate the water-leaving radiance. This radiance received by the sensor at the TOA in a spectral wavelength centered at a wavelength λ , ($L_t(\lambda)$), is considered to be in absence of wind-generated oceanic whitecaps or foam, and for viewing directions out of the sun glint (i.e., the direction of specular reflection of sunrays by a more or less wavy interface) and can be split into the

following components:

$$L_t(\lambda) = L_a(\lambda) + L_r(\lambda) + t_d(\lambda).L_w(\lambda) \quad (1)$$

- Where, L_t is sensor-detected radiance;
- L_a is aerosol path radiance = $F_o \omega_{oa} \tau_a P_a / 4\pi \cos \theta_v$;
- L_r is Rayleigh path radiance = $F_o \omega_{or} \tau_r P_r / 4\pi \cos \theta_v$;
- L_w is water-leaving radiance;
- ω_{oa} is aerosol scattering albedo;
- ω_{or} is Rayleigh single scattering albedo;
- θ_v is satellite viewing zenith angle;
- τ_a / τ_r is Aerosol/Rayleigh optical depth;
- P_a / P_r is aerosol/Rayleigh scattering phase function;
- t_d is atmospheric diffuse transmittance = $\exp[-(1/\cos \theta_v + 1/\cos \theta_s)(\tau_r(\lambda)/2 + \tau_{oz}(\lambda))]$;
- θ_s is solar zenith angle and
- τ_{oz} is Ozone absorption optical depth.
- F_o is the extraterrestrial solar flux.

In eq. (1), both Rayleigh radiance and aerosol path radiance constitute the atmospheric path radiance. The aerosol phase function is determined using Heyney–Greenstein model (Gordon 1997). The Rayleigh path radiance is computed as the spectral dependence of the Rayleigh optical depth, and the Rayleigh phase functions are well known. The diffuse transmittance is also computed from the Rayleigh optical depth and ozone absorption optical depth. The value of the ozone absorption optical depth is taken as constant, since its variation within the spectral range of ocean-colour sensor is negligible. The water-leaving radiance component for

wavelengths above 700nm is very small for open ocean clear waters due to strong infrared absorption by water. Aerosol path radiance is calculated from the Rayleigh corrected TOA radiance at 765 and 865 nm wavelengths. While, for wavelengths (< 700nm), the aerosol path radiance is computed through extrapolation method as discussed by Chauhan et. al., (2002) for OCM.

Standard atmospheric correction algorithm works well for open ocean water, but fails when extended and used over coastal turbid waters due to significant water-leaving component at 765 and 865nm wavelength in these regions. This leads to severe overestimation of the aerosol radiances and negative water-leaving radiances for 412nm and 443nm in these regions. To overcome this problem, the approach suggested by Wang, (2007); Wang et. al., (2007, 2009) has been adopted to perform turbid water atmospheric correction for MODIS data over Arabian Sea using shortwave infrared (SWIR) wavelengths where, the absorption by water is extremely high so that even turbid productive waters can be safely presumed to have zero reflectance. Penetration depths of sunlight into the water for the longer wavelengths (1.2, 1.6, and 2.1 μm) are very small, eliminating the possibility of the reflection by sediments as shown in figure 2. Therefore, with the black ocean assumption at the SWIR wavelengths, these can be used for detecting turbid waters as well as for atmospheric correction in the coastal ocean regions. SWIR atmospheric correction algorithm is performed using the SWIR wavelength set of 1240 and 2130 nm and the aerosol path radiance is calculated from the Rayleigh corrected TOA radiance at these wavelengths. Aerosol path radiance for wavelengths (< 1240nm) of the MODIS, were computed through simple extrapolation method using SWIR spectral

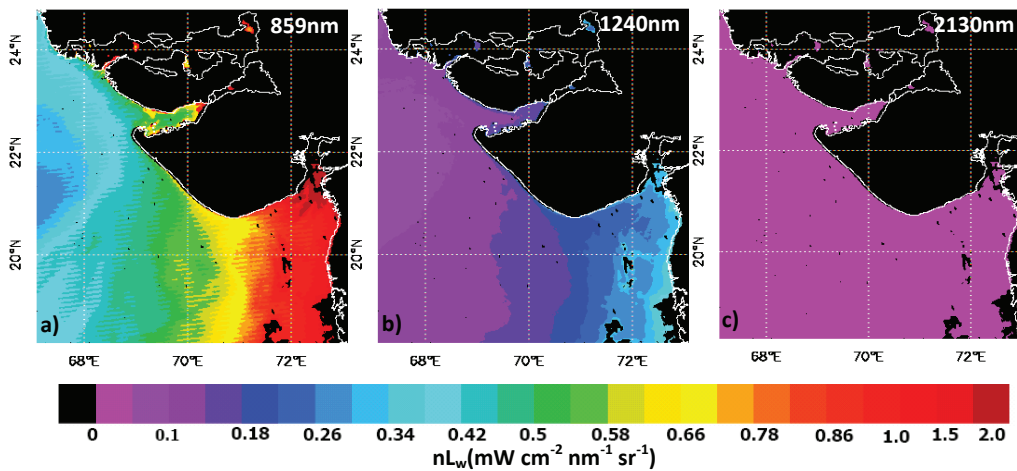


Figure 2. The TOA radiance measured by MODIS-Aqua at wavelengths (a) 859 nm, (b) 1240 nm, and (c) 2130 nm on October 17, 2007 for the coastal region along Gujarat, India.

model for its wavelength variation. On removing these new aerosol components from the total radiance at the desired wavelength and dividing it by the atmospheric transmittance, the corresponding water-leaving radiances were obtained.

5. Results and discussions

The assumption of zero water-leaving radiance (L_w) at NIR wavelengths has been replaced by zero L_w at SWIR wavelengths which means the ocean is totally absorbing at

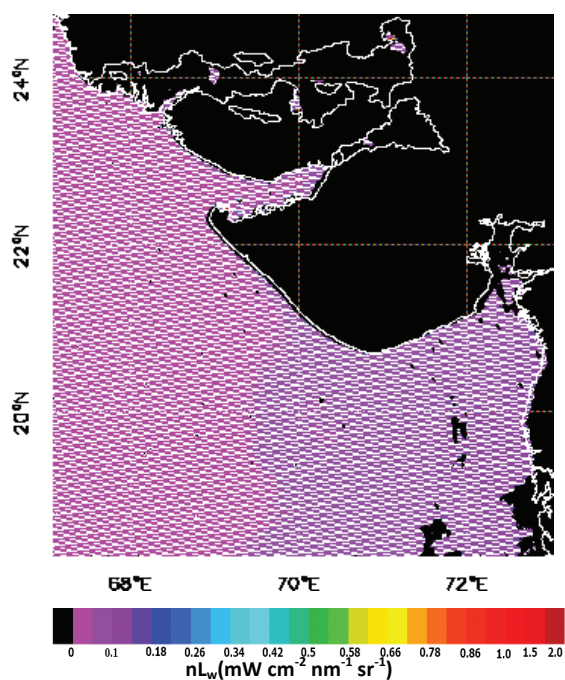


Figure 3. The TOA radiance measured by MODIS-Aqua at wavelengths 1640 nm on October 17, 2007 for the coastal region along Gujarat, India.

these wavelengths, and this forms the basis for the correction of aerosol path radiance (L_a). Hale and Query (1973), showed that the water absorption coefficients for wavelengths 865, 1240, 1640, and 2130 nm are approximately 5, 88, 498, and 2228 m^{-1} , respectively. Therefore, SWIR wavelengths were used for atmospheric correction in the coastal ocean regions with the black ocean assumption at these wavelengths. However, for MODIS-Aqua, some detectors for the SWIR 1640 nm wavelength are inoperable and cannot be used effectively as shown in figure 3. Hence, SWIR atmospheric correction algorithm was performed using the SWIR wavelength set of 1240 nm and 2130 nm are evaluated. Aerosol optical depth at NIR band with central wavelength at 859nm computed with radiance at wavelengths $> 1240nm$ and with the help of SWIR spectral model is shown in figure 4. On removing aerosol components from the total radiance at the desired wavelength and dividing it by the atmospheric transmittance, the water-leaving radiances at visible wavelengths were obtained using simple extrapolation method with SWIR spectral model. The water-leaving radiances obtained using NIR wavelengths in standard atmospheric correction and SWIR wavelengths in new atmospheric correction approach are shown in figure 5. The arrows pointing the dark areas in Figure 5 (left) shows the negative values obtained for coastal turbid waters using NIR scheme while rest of the dark area in figure 5 (both right and left) denotes the land and cloud mask. Changes in water-leaving radiance spectra derived using the SWIR channel approach relative to their standard atmospheric correction counterparts are shown in figure 6. The modified atmospheric correction led to gains in water-leaving radiance at all wavelengths compared to standard atmospheric corrected values. MODIS derived normalized water leaving radiance using both the algorithms for wavelengths 412nm, 442nm, 488nm, 531nm, 555nm and 645nm have also been compared with *in-situ* measured normalized water-leaving radiance for twelve coastal stations as shown in figure 7 and figure 8.

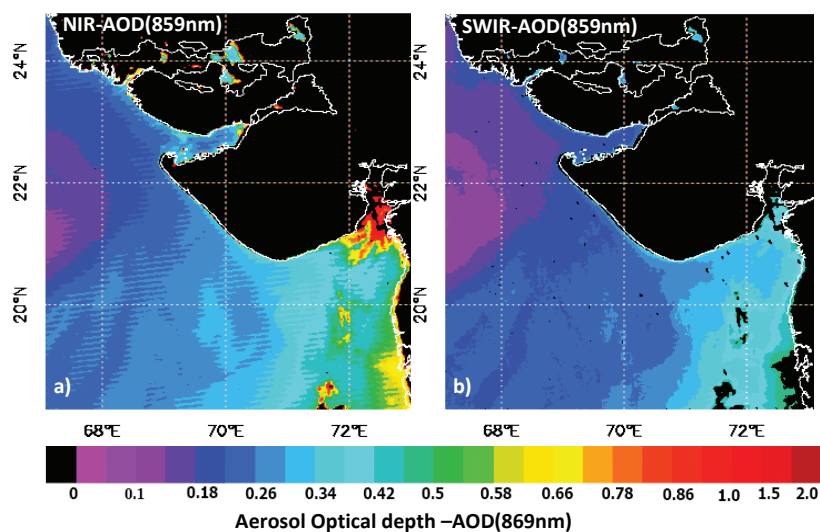


Figure 4. MODIS-Aqua derived Aerosol Optical Depth (AOD) at 859 nm a) after Standard Atmospheric Correction b) after SWIR Atmospheric correction on October 17, 2007 for the coastal region along Gujarat, India.

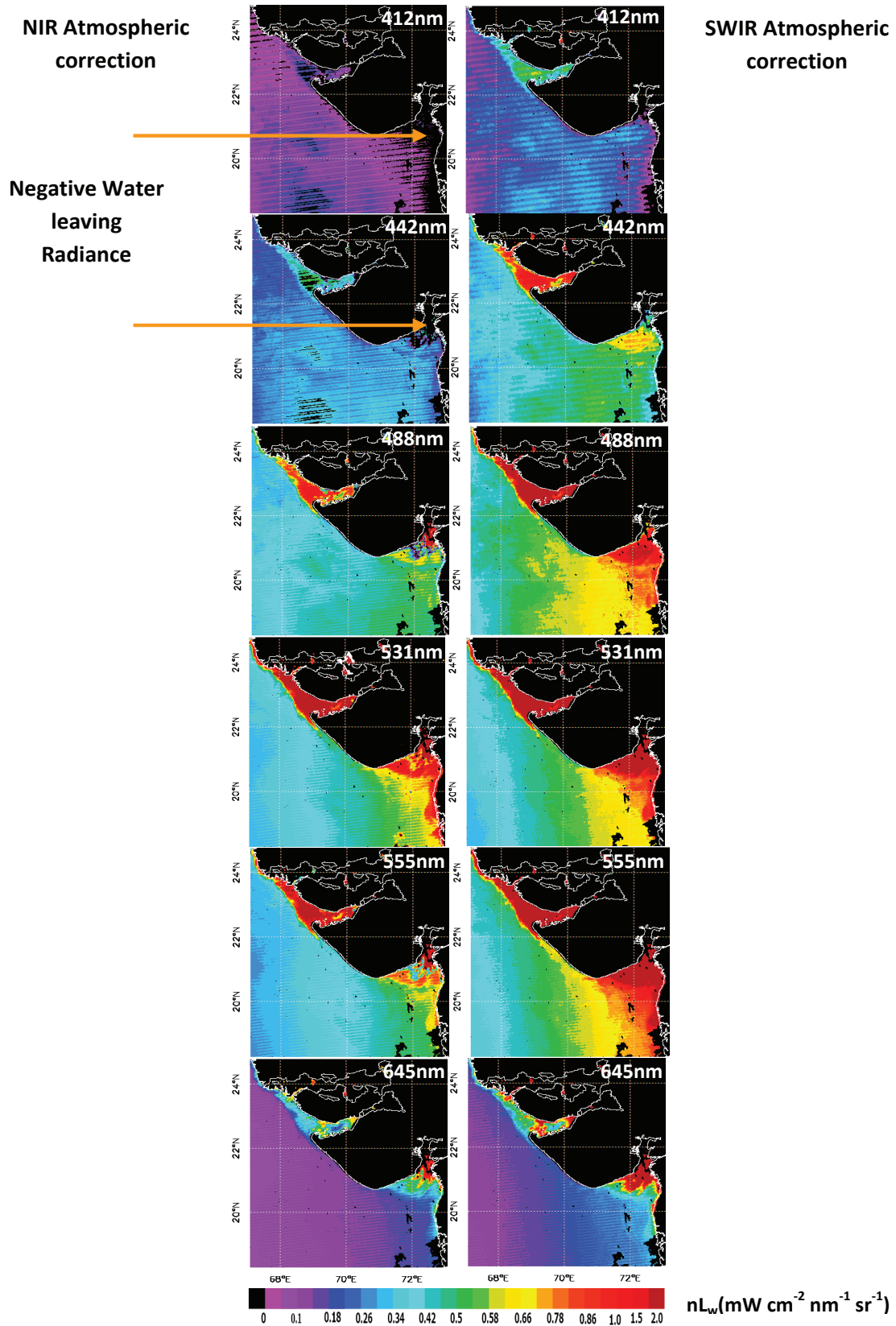


Figure 5. Normalized Water-leaving radiance after Standard Atmospheric Correction (Left) and after SWIR Atmospheric correction (Right) for MODIS-Aqua bands for the coastal region along Gujarat, India.

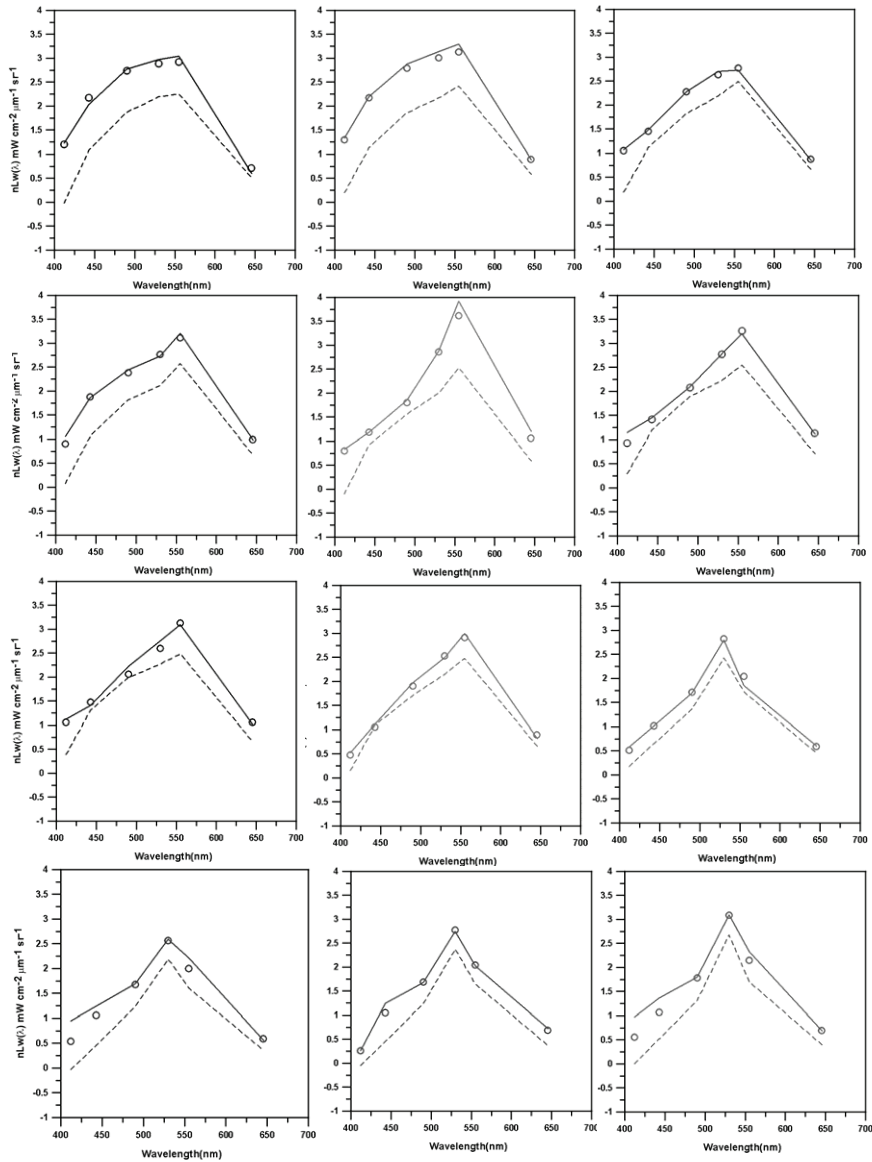


Figure 6. Normalised water-leaving radiance spectra shown by i) dotted line for standard atmospheric correction, ii) circles for SWIR atmospheric correction and iii) by solid line for *in-situ* measurements for different cruise locations.

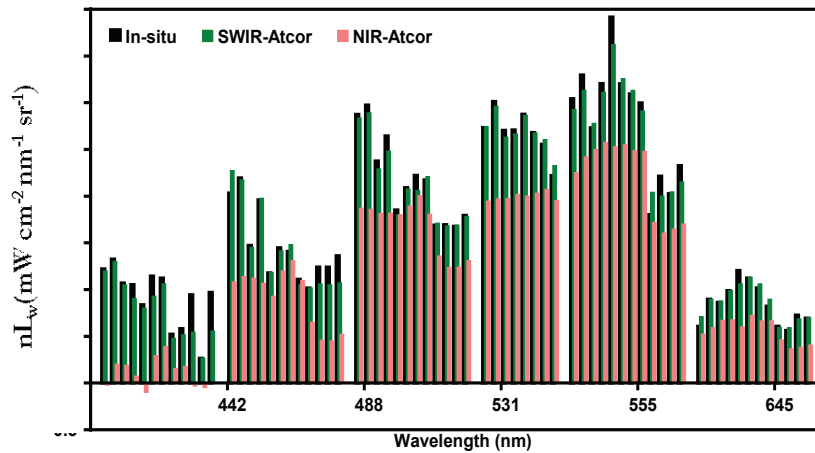


Figure 7. Comparison of *in-situ* measured and satellite derived normalized water leaving radiance using standard atmospheric correction and SWIR atmospheric correction.

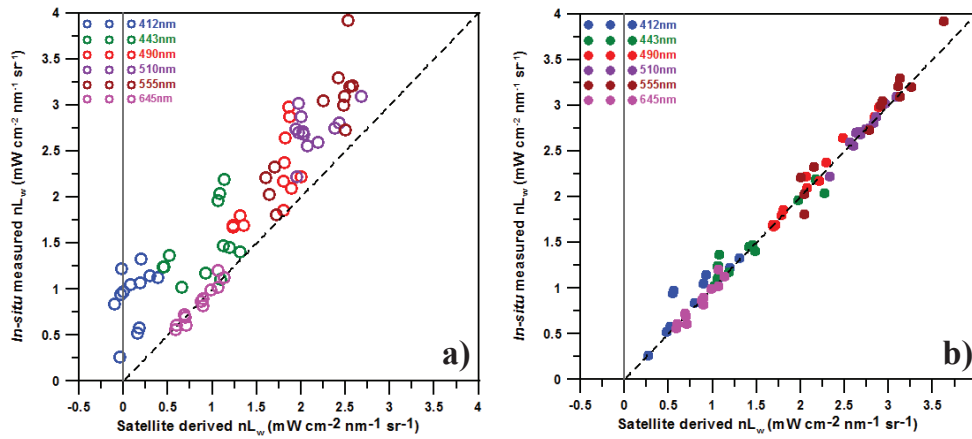


Figure 8. Regression between the *in-situ* measured and estimated normalised water leaving radiance for a) standard atmospheric correction and b) SWIR atmospheric correction.

Results of regression between the *in-situ* measured and satellite derived normalized water leaving radiance using both the methods are tabulated in table 1. The variation in terms of percentage difference between the *in-situ* and satellite derived water-leaving radiance for different wavelengths have also been tabulated in Table 1. It is to note here that a very high % error of ~89.5 and 36.3 for 412nm and 443nm with RMSE of 0.31 and 0.36 are observed due to the negative water leaving radiance in these channels. The underestimation of radiance values by the use of NIR channel procedure over coastal turbid waters at these wavelengths has been considerably reduced using SWIR channels. Percentage error was limited to ~13.0 and 3.7 with RMSE of 0.15 and 0.11 for 412nm and 443nm respectively. Comparison of *in-situ* and satellite derived water leaving radiance (of all wavelengths) in figure 6 and 7 also exhibits an improvement over the NIR channel procedure in terms of the correlation coefficient r^2 , which was increased to 0.98 using SWIR channel approach than $r^2= 0.86$ of NIR channel in standard atmospheric correction.

6. Conclusions

Standard atmospheric correction algorithm fails when extended and used over coastal turbid waters. The assumption of zero water-leaving radiance (L_w) at NIR wavelengths has been therefore replaced zero water-leaving radiance at highly absorbing SWIR wavelengths. Physically realistic and positive water leaving radiances throughout the spectrum and especially for shorter wavelengths (412nm, 443nm, 490nm) were obtained over coastal turbid waters using this concept. The results of the turbid water atmospheric correction have also been validated for twelve coastal stations using *in-situ* measured water-leaving radiance. Variation between the *in-situ* measured and satellite derived water leaving radiance for wavelengths 412nm, 443nm, 490nm, 512nm and 555nm was found to be considerably reduced by the use of SWIR wavelengths for atmospheric correction and the correlation coefficient arrived at 0.98, which is as an improvement over the standard atmospheric correction procedure.

Table 1. Results of regression analysis between the *in-situ* measured and satellite derived normalized water leaving radiance for different wavelengths.

Wavelength (nm)	Slope	Intercept	r^2	RMSE	%diff
Standard Atmospheric Correction Algorithm					
412	0.69	0.85	0.11	0.31	89.48
442	0.57	0.95	0.21	0.36	36.32
488	1.15	0.25	0.52	0.34	22.23
531	0.43	1.80	0.21	0.21	25.39
555	1.32	-0.09	0.76	0.32	20.98
645	1.25	0.14	0.58	0.14	32.56
All	1.005	0.56	0.86	0.33	38.54
SWIR Atmospheric Correction Algorithm					
412	0.87	0.23	0.80	0.15	12.98
442	0.80	0.32	0.93	0.11	3.68
488	1.07	-0.09	0.98	0.06	1.96
531	1.11	-0.29	0.96	0.05	0.26
555	1.07	-0.14	0.95	0.15	1.79
645	1.07	-0.07	0.92	0.06	-1.36
All	0.99	0.065	0.98	0.12	3.36

Acknowledgements

This work is supported under the Meteorology and Oceanography (MOP) program of Indian Space Research Organisation (ISRO). Two authors Nivedita Sanwani and Prakash Chauhan are thankful to Dr. Ajai, Group Director, MESG and Dr. J.S. Parihar, Deputy Director, RESA of Space Applications Center (ISRO), Ahmedabad for their valuable advice and encouragement.

References

- Antoine, D., & Morel, A., (1999). A multiple scattering algorithm for atmospheric correction of remotely sensed ocean colour (MERIS instrument): Principle and implementation for atmospheres carrying various aerosols including absorbing ones. *International Journal of Remote Sensing*, 20, 1875–1916.
- Chauhan, P., Mohan, M., Sarangi, R. K., Kumari, B., Nayak, S., & Matondkar, S. G. P., (2002). Surface chlorophyll estimation in the Arabian Sea using IRS-P4 OCM Ocean Color Monitor (OCM) satellite data. *International Journal of Remote Sensing*, 23(8), 1663–1676.
- Esaias, W., (1998). An Overview of MODIS Capabilities for Ocean Science Observations. *IEEE Transaction of Geoscience of Remote Sensing*, 36, 1250–1265.
- Gao, B. C., Montes, M.J., Ahmad, Z., and Davis C. O., (2000). Atmospheric correction algorithm for hyperspectral remote sensing of ocean color from space. *Applied Optics*, 39, 887-896.
- Gordon, H.R., Wang, M., (1994). Retrieval of water-leaving radiance and aerosol optical thickness over the oceans with SeaWiFS: a preliminary algorithm. *Applied Optics*, 33, 443-452.
- Gordon, H. R., (1997), Atmospheric correction of ocean colour imagery in the Earth Observing System era, *Journal of Geophysical Research*, 102, 17081-17106.
- Hale, G. M., & Querry, M. R., (1973). Optical constants of water in the 200nm to 200 μ m wavelength region. *Applied Optics*, 12, 555–563.
- Hu, C., Carder, K. L., and Muller-Karger, F. E., (2000). Atmospheric correction of SeaWiFS imagery over turbid coastal waters: a practical method. *Remote Sensing of Environment*, 74, 195-206.
- Jamet, C., Moulin, C. and Thiria, S., (2004). Monitoring aerosol optical properties over the Mediterranean from SeaWiFS images using a neural network inversion. *Geophysical Research Letters*, 31, L13107.
- Land, P.E. and Haigh, J.D., (1996). Atmospheric correction over case2 waters with an iterative algorithm. *Applied Optics*, 35, 5443-5451.
- Lavender, S.J., Pinkerton, M.H., Moore, G.F., Aiken, J. and Blondeau-Patissier, D., (2005). Modifications to the atmospheric correction of SeaWiFS ocean colour images over turbid waters. *Continental Shelf Research*. 25, 539-555.
- Li, R. R., Kaufman, Y. J., Gao, B. C., & Davis, C. O., (2003). Remote sensing of suspended sediments and shallow coastal waters. *IEEE Transactions on Geoscience and Remote Sensing*, 41, 559–566.
- Moore, G., Aiken, J. and Lavender S., (1999). The atmospheric correction of water colour and the quantitative retrieval of suspended particulate matter in Case II waters: application to MERIS. *International Journal of Remote Sensing*, 20(9), 1713-1733.
- Morel, A., & Belanger, S., (2006). Improved detection of turbid waters from ocean color sensors information. *Remote Sensing of Environment*, 102, 237–249.
- Morel, A., (1980). In-water and remote measurement of ocean colour, *Boundary-Layer Meteorology*, 18, 177-201.
- Nobileau, D., & Antoine, D., (2005). Detection of blue-absorbing aerosols using near infrared and visible (ocean color) remote sensing observations. *Remote Sensing of Environment*, 95, 368–387.
- Ruddick, K.G., Ovidio, F. and Rijkeboer, M., (2000). Atmospheric correction of SeaWiFS imagery for turbid coastal and inland waters. *Applied Optics*, 39, 897-912.
- Schroeder, Th., Fischer J., Schaale M. and Fell, F., (2003). Artificial Neural Network based atmospheric correction algorithm: Application to MERIS data, Free University Berlin.
- Seigel, D.A., Wang, M., Maritorena, S. and Robinson, W., (2000) Atmospheric correction of satellite ocean colour imagery: the back pixel assumption. *Applied Optics*, 39, 3582-3591.
- Sturm, B., (1980). The atmospheric correction of remotely sensed data and the quantitative determination of suspended matter in marine water surface layers. *Remote Sensing in Meteorology, Oceanography and Hydrology*, A. P. Cracknell, ed. (Ellis Horwood, Chichester, UK, 1980), 163-197.
- Torres, O., Herman, J. R., Ahmad, Z., and Gleason, J., (1998). Derivation of aerosol properties from satellite measurements of backscattered ultraviolet radiation: Theoretical basis. *Journal of Geophysical Research*, 103, 17,099–17,110

- Viollier, M., Tanre, D., and Deschamps, P.Y., (1980). An algorithm for remote sensing of water colour from space. *Boundary-Layer Meteorol.* 18, 247-267.
- Wang, M., & Shi, W. (2007). The NIR-SWIR combined atmospheric correction approach for MODIS ocean color data processing. *Optics Express*, 15, 15722–15733.
- Wang, M., Son, S., & Shi, W. (2009). Evaluation of MODIS SWIR and NIR-SWIR atmospheric correction algorithm using SeaBASS data. *Remote Sensing of Environment*, 113, 635–644.
- Zhang, T., Fell, F. and Fischer, J., (2002). Modeling the backscattering ratio of marine particles in case-2 waters. *Proceedings of the Ocean Optics XVI*, Santa Fe, USA, published on CDROM.